Russian Journal of Earth Sciences Online ISSN: 1681-1208

Special Issue: "Kamchatka Earthquake M 8.8 on July 29, 2025"

Seismic Monitoring in Severo-Kurilsk Before and After the July 29 (30), 2025 Earthquake Based on Data from an Engineering Seismometric Station

N. V. Kostyleva[1,2,*] and D. V. Kostylev[1,2]

[1]Institute of Marine Geology and Geophysics of the FEB RAS, Yuzhno-Sakhalinsk, Russian Federation
[2]Sakhalin Branch of the Geophysical Survey of RAS, Yuzhno-Sakhalinsk, Russian Federation
* **Correspondence to:** Natalia Kostyleva, n.kostyleva@imgg.ru

Abstract: In April 2024, an engineering seismometric station was installed in a residential building in Severo-Kurilsk (Paramushir Island, Sakhalin Oblast) to obtain information about the vibrations of structures and adjacent ground areas during earthquakes as part of seismic observations conducted by the Sakhalin Branch of the Geophysical Survey of the Russian Academy of Sciences. Based on the obtained data on the intensity of the Kamchatka earthquake of July 29 (30), 2025, $M_W = 8.8$, in residential buildings in Severo-Kurilsk, the development of the seismic process before and after the earthquake was analyzed. The obtained data were compared with data from a stationary seismic station in Severo-Kurilsk, located 900 m from the residential building. Both stations are equipped with strong vibration sensors installed in different conditions. Of the 1,790 earthquakes (with a magnitude of $M \geq 3.5$) recorded by the regional seismic network from July 29 to October 15, 2025, 195 events with an intensity of $I \geq 3.6$ impacted residential buildings. Of these 195 earthquakes, 14 had an impact magnitude of $I \geq 6.0$, and the main directions of the axes of maximum impact on residential buildings were east–west and north–south. The study results demonstrate that integrating engineering and technical monitoring into the urban environment is an important element of seismic risk reduction strategies and operational decision-making after strong earthquakes.

Keywords: Engineering seismometric station, seismic process, accelerometer, instrumental intensity, Kamchatka megathrust earthquake

Citation: Kostyleva N. V. and Kostylev D. V. (2026), Seismic Monitoring in Severo-Kurilsk Before and After the July 29 (30), 2025 Earthquake Based on Data from an Engineering Seismometric Station, *Russian Journal of Earth Sciences*, 26, ES2016, EDN: NTCQEA, https://doi.org/10.2205/2026es001126

Research Article

Received: February 2, 2026
Accepted: May 25, 2026
Published: July 1, 2026

1. Introduction

An engineering seismometric station is an instrumentation system for recording the movement of building or structure elements and adjacent ground areas during earthquakes. It incorporates seismometric equipment (primary transducers) installed directly on the building or structure elements, as well as on the ground near the observation site, as well as the equipment and facilities of the processing center and communication channels. Information obtained from the integrated seismic system is used in both the theory and practice of earthquake engineering, including for engineering assessments of earthquake intensity. Code of Practice (SP 330.1325800.2017) "Buildings and Structures in Seismic Areas. Design Rules for Engineering Seismometric Stations" (in Russia since 2018) establishes requirements for equipping buildings and structures in seismic areas with engineering seismometric stations (ESS). Such stations, first and foremost, allow for the most rapid and accurate assessment of the impact on a specific monitoring site (rather than across the entire territory). This allows relevant agencies, in the event of a strong earthquake, to obtain information on the need for specific measures and determine the timeframe for their implementation (rescue, evacuation, reinforcement, repair, etc.). Furthermore, in cases of constant exposure of operational facilities to seismic vibrations of relatively low intensity, fatigue phenomena occur in structural materials, accompanied by the accumulation of internal damage and leading to changes in the physical condition of the structures. In particular, a change in the natural frequency of vibrations (determined by the ESS) may indicate changes in the monitoring site, such as changes in the strength of the facility or the nature of the connections between its components.

Currently, independent observations using integrated seismic systems are being conducted at branches of the Geophysical Survey, Russian Academy of Sciences (GS RAS). Specifically, such observations have begun at the Kamchatka Branch (KB) of GS RAS [*Chebrov et al.*, 2021], and since 2024, they have also been conducted by the Sakhalin Branch (SB) of GS RAS. To obtain primary information on the nature of seismic impacts on construction sites, integrated seismic systems were installed on urban buildings in populated areas of the Sakhalin Oblast (in populated areas on Shikotan Island and in the city of Severo-Kurilsk on Paramushir Island) [*Kostylev and Kostyleva*, 2025a]. Operational values of the intensity of object vibrations are determined based on the maximum values of peak accelerations at the monitoring site during an earthquake using instrumental methods, according to [*Droznin et al.*, 2018]. The information obtained is particularly important in the event of a strong earthquake, since the Earthquake Early Alert Service (EEAS) provides a summary only of the main parameters of a seismic event, which require additional interpretation. In cases of constant exposure of operational facilities to seismic vibrations of relatively low intensity, fatigue phenomena occur in structural materials, accompanied by the accumulation of internal damage and leading to changes in the physical condition of the structures. EEAS data is used to monitor the condition of buildings, since such damage is not always visually detectable and can lead to the self-destruction of structures [*Guryev et al.*, 2023]. The aim of the work is to use the example of the strongest earthquake on July 29 (30), 2025 with $M_W = 8.8$ [*Chebrov*, 2025], which occurred near the Kamchatka Peninsula, to demonstrate the capabilities of the ESS in Severo-Kurilsk and to assess the dynamics of seismic activity before and after the event based on the information received on the instrumental intensity of the impact of earthquakes on the residential building stock of Severo-Kurilsk.

2. Materials and Methods

In 2024, the SB GS RAS developed a system for assessing seismic impacts on construction sites based on the integrated seismic systems installed on urban buildings. The system complies with regulatory document (SP 330.1325800.2017). The ESS hardware includes Russian-made equipment: the MTSS-1033A molecular-electronic accelerometer, included in the state register of measuring instruments, integrated with the NDAS-8426N recorder. Such ESS systems enable continuous monitoring of the site in near-real time, detecting seismic events, and sending messages to the system operator [*Titov et al.*, 2021]. According to BBP-20 uninterruptible power supplies with 7 Ah batteries are used to ensure uninterruptible power supply. Real-time data transmission is carried out via cellular communication channels. In addition to data transmission, the system's functionality allows for the detection and processing of events of varying intensity based on built-in triggers, as well as, based on the received data, the prompt management of local security systems (elevator equipment, gas systems, sound alarms, etc.).

The monitoring facility is a three-story, monolithic building with 24 apartments, built in 2019. The building has a reinforced concrete foundation, floors, and interior walls, while the exterior walls are made of aerated concrete blocks. The roof is metal tile. The building's structural design is frameless with cross-supporting walls. All joints between the foundations and the walls and between the walls and the floor slabs ensure the stability and rigidity of both the individual structures and the building as a whole. The ESS recording device is installed in the building's attic on a 240 mm thick monolithic reinforced concrete floor slab, supported by internal and external load-bearing monolithic reinforced concrete walls, which are rigidly connected to the floor (Figure 1).

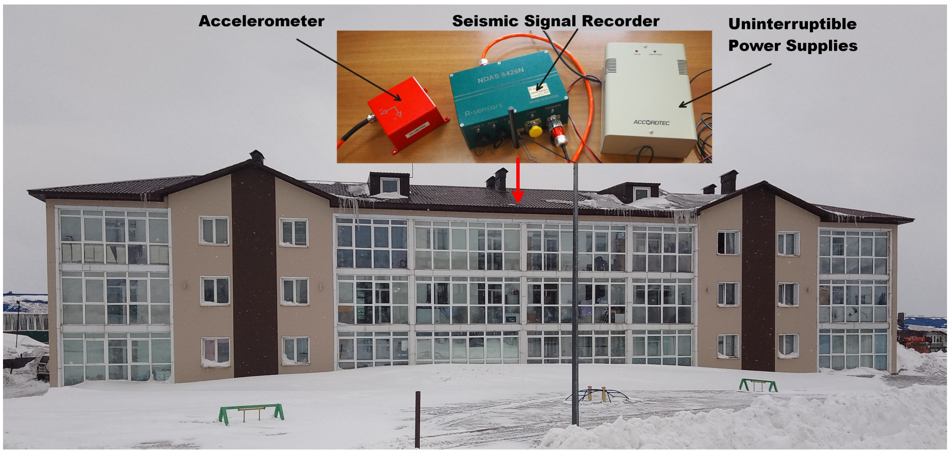

Figure 1. Installation of recording equipment in one of the residential buildings in Severo-Kurilsk.

Based on the system described above, the ESS in a residential building in Severo-Kurilsk (hereinafter referred to as the monitoring facility) was commissioned on April 1, 2024. The ESS in Severo-Kurilsk is integrated into the unified data collection network of the SB GS RAS [*Kostylev*, 2021] in real time, enabling its data to be used, among other things, for seismic event localization at the Yuzhno-Sakhalinsk Regional Operational Center [*Kostylev and Kostyleva*, 2025b].

In addition to the ESS, in accordance with the SP, in the city of Severo-Kurilsk, in the immediate vicinity of the monitoring facility of the SB GS RAS, there is a permanent seismic station "Severo-Kurilsk" (station code SKR). The distance to the monitoring facility is 900 m. It was opened on March 1, 1958 as a class 1 station, part of the Unified Seismological Observation System of the USSR and performing tsunami warning tasks based on seismological data. Since March 27, 2009, it has been equipped with digital equipment and included in the unified seismological information collection system of the SB GS RAS. It is a reference station of the seismic subsystem of the Tsunami Warning Service [*Chebrov et al.*, 2010]. Soil – loose sandstone. Currently, the station uses equipment from Guralp – a broadband borehole seismometer Guralp CMG-3TB and an accelerometer Guralp CMG-5T, connected to a seismic signal recorder Guralp CMG-DAS-S6 [*Mishatkin et al.*, 2012]. The accelerometer is installed in the heated seismic pavilion of the Severo-Kurilsk station on a pedestal made of a concrete pillar measuring 1.5 m × 1.5 m × 2.0 m, reinforced with pipes driven into the ground. The pedestal is 50 cm above the floor and is embedded 1.5 m deep, which is below the ground freezing level in Severo-Kurilsk.

2.1. Methodology for Assessing the Intensity of Tremors

Waveforms arriving at the Yuzhno-Sakhalinsk Regional Operational Center in near real-time are processed using the DIMAS software package developed at the KB GS RAS and designed for detailed processing and visual analysis of digital seismic signals coming from various acquisition systems [*Droznin and Droznina*, 2011]. Further, to estimate the actual intensity of shaking based on instrumental data, a certain relationship is used, given in the draft of the new Russian seismic scale [*Aptikaev et al.*, 2011], which was developed based on the MSK-64 scale [*Medvedev et al.*, 1964] and its modifications. The equation linking seismic intensity in points with such a ground motion parameter as acceleration according to [*Aptikaev et al.*, 2011] is as follows:

$$I = 2.5 \lg \mathrm{PGA} + 1.89,$$

where I is the shaking intensity; PGA is the peak ground acceleration.

The rapid response to shaking intensity and impact on a residential building begins at an intensity of 3.6. This rating corresponds to the classification adopted in the MSK-64 scale "Intensity IV. Noticeable Shaking," when an earthquake begins to impact the stability of the building itself. A summary of shaking intensity data is provided to relevant agencies promptly, as well as in monthly reports.

From the commissioning of the ESS in Severo-Kurilsk on April 1, 2024, through July 29 (30), 2025, the instrumental intensity exceeded 3.6 (I=3.6) for only nine seismic events. The maximum intensity of the events that occurred was I = 6.3 for the ESS in Severo-Kurilsk (October 23, 2024). The epicenters of the earthquakes are shown in Figure 2.

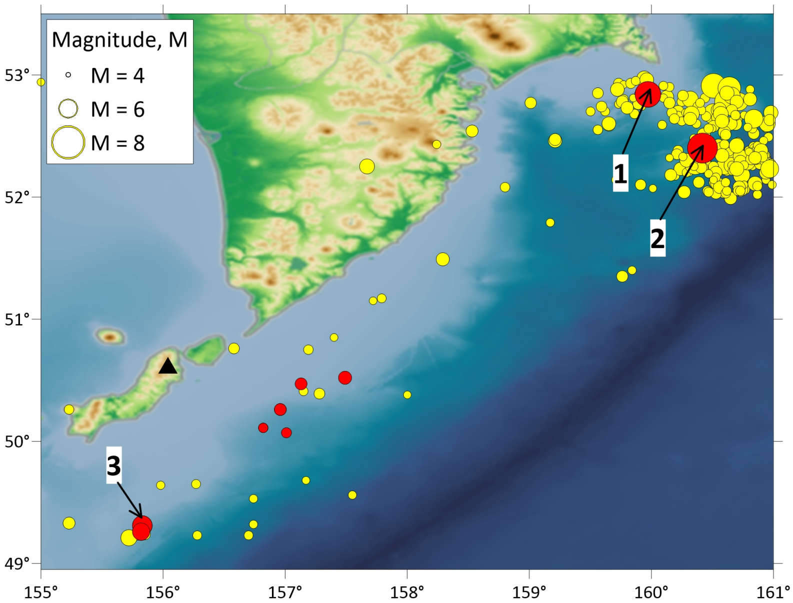

Figure 2. On the left are the epicenters of all seismic events with $M \geq 3.5$ from April 1, 2024 to July 29, 2025. Earthquakes with $I \geq 3.6$ according to the ESS instrumental data at the monitoring site in Severo-Kurilsk (black triangle) are highlighted in red. The numbers indicate the strongest earthquakes during the observed period: 1 – August 17, 2024 with M_W = 7.0; 2 – July 20, 2025 with M_W = 7.7; 3 – October 23, 2024 with M_W = 6.0.

Strong seismic events 1 and 2, which occurred near the Kamchatka Peninsula, despite their magnitudes, had a weak impact on the monitored object, and their aftershock sequences had no impact at all. However, earthquake 3 south of Paramushir Island had a macroseismic effect I = 6.3 on the residential building of interest, most likely due to the close epicentral distance from the island.

3. Results and Discussion

The earthquake of July 29 (30), 2025, and its subsequent aftershocks had a strong, in places destructive, impact on the town of Severo-Kurilsk and the island of Paramushir as a whole. An 8-meter-high tsunami struck the coastal part of the island, forcing residents to higher ground [*Kostenko et al.*, 2025]. The town's port and fishing facility were flooded. About 15 unmanned vessels of varying sizes were washed out to sea from the port area. According to district authorities, 121 structures were damaged in Severo-Kurilsk – all residential buildings (106 buildings), social and municipal infrastructure. These included the buildings of a kindergarten, school, community center, children's art school, museum and library, city bathhouse, pharmacy, etc. (https://www.kommersant.ru/doc/7944030).

In addition to a visual impact assessment, it would be appropriate to conduct an assessment using seismic instrument recordings from Severo-Kurilsk based on peak acceleration values at the monitoring site and the Severo-Kurilsk seismic station. The results obtained will allow for a more detailed assessment of the impact of the seismic event and its aftershocks on the town.

The first earthquake (the main shock) occurred on July 29 at 23:24 UTC (July 30 at 10:24 Sakhalin Time). Less than two minutes later, a recording of the earthquake appeared on the monitors of the duty operators of the Yuzhno-Sakhalinsk Regional Operational

Center. Just six minutes later, based on operational data processing, the duty officer transmitted a message to the Tsunami Center and the Crisis Management Center of the Main Directorate of the Ministry of Emergency Situations of the Russian Federation for the Sakhalin Region. Ten minutes later, a tsunami alert was issued for the Severo-Kurilsk District. Figure 3 shows the information message from the SB GS RAS with earthquake parameters and the time of data transmission to the Rapid Response Centers.

INFORMATION MESSAGE SB GS RAS

Earthquake 2025.07.29 23:24:49 UTC
Coordinates 52.4°N 160.6°E
Depth 9 km
Magnitude 8.3
142 km east of Petropavlovsk-Kamchatsky
278 km east of Pauzhetka
2025.07.29 23:29:04 UTC
Grigorieva

CC:

R: 23-27-52 GMT
Proc. Kim
Rec. Naumova 10-30 Sakhalin time

CESC/CC:

July 30 10-24 Sakhalin time Earthquake
Coord. 52.4°N 160.6°E
H= 10 km
M= 7.9
TSUNAMI WARNING ISSUED for North Kuril District!
Proc. Grigorieva
Rec. Troshin 10-40 Sakhalin time
Rec. Naumova 10-42 Sakhalin time

Figure 3. Screenshot of the information message about the earthquake, generated by the duty shift of the Yuzhno-Sakhalinsk Regional Operational Center after the operational processing of the registered seismic event. (Translated from Russian for this publication.)

Figure 4 presents data on the earthquake's impact time and spectral composition as recorded by the recording equipment at the Severo-Kurilsk seismic station and the monitoring site built by the authors in the DIMAS software package. Calculation of the instrumental intensity based on peak acceleration data (PGA) of ground displacement at the installation site of the seismic station in Severo-Kurilsk and at the monitoring site showed $I = 9.1$ on the Seismic Intensity Scale (GOST R 57546-2017).

The figure below shows the instrumental intensity plots based on the PGA values at each station. It is clear that the instrumental intensity values are consistent.

A total of 1,790 seismic events with $M \geq 3.5$ were recorded from July 29 to October 15 [*Kostylev et al.*, 2025], of which 195 events had an impact on the monitored object with an intensity greater than 3.6. Figure 5 shows all recorded events for the observed period (upper part of the figure). The 195 earthquakes with an instrumental intensity of $I \geq 3.6$ are highlighted in red. The lower part of the figure shows the distribution of aftershocks by the time of their occurrence.

All 195 earthquakes with instrumental intensities of $I \geq 3.6$ are presented separately in Figure 6, but with detailing by intensity level. As can be seen from the figure, most had instrumental intensities no higher than $I = 4.9$, but many seismic events were felt much more strongly by the population. According to the results of a regularly conducted macroseismic survey among the population, most of the earthquakes shown in Figure 6 were felt by the population (according to the MSK-64 scale) much more strongly than the instrumental intensity values indicated. Earthquakes occurring east of 158°E had a less noticeable impact on Paramushir Island despite their high magnitudes. However, the macroseismic impact from earthquakes occurring in the longitude range of 156°–158°E was more powerful despite very low magnitudes. For example, earthquakes with $M \geq 5.5$ occurring in this range caused tremors of intensity 7. This fact can most likely be explained by the geological features of the region's structure. It is worth noting that the majority of felt earthquakes are concentrated in the immediate vicinity of Paramushir Island. From this we can conclude that earthquakes occurring to the east of 158°E have a serious macroseismic

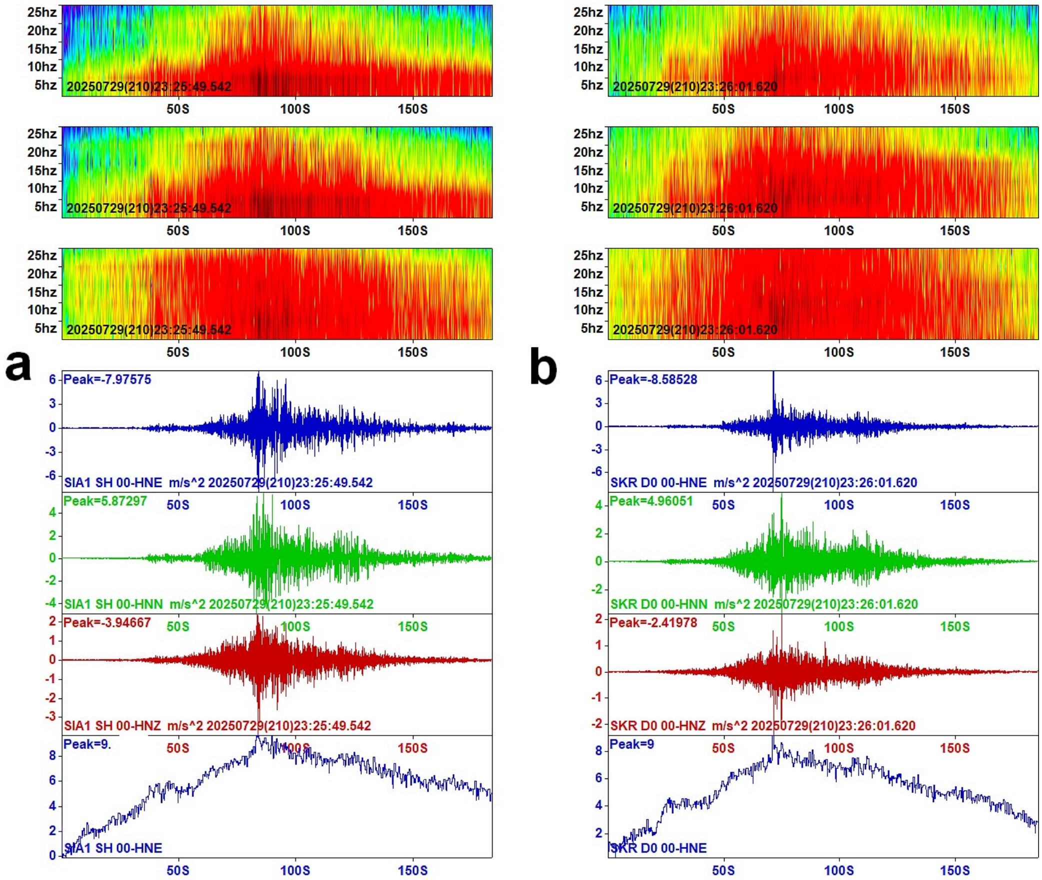

Figure 4. Spectral composition of the main shock and its waveforms; (*a*) at the monitoring site, (*b*) at the Severo-Kurilsk seismic station.

impact on the city of Severo-Kurilsk with a magnitude of $M \geq 7.0$, while the main impact is caused by seismic events in the range of 156°–158°E.

To demonstrate the relationship between the number of registered events and their intensity, a distribution diagram of perceptible ($I \geq 3.6$) events over time was constructed (Figure 7). The diagram essentially represents a graph of aftershock decay. The graph clearly shows how, as the total number of events attenuates (orange line), earthquakes with $I = 7.0$ can be observed in the city of Severo-Kurilsk, as these aftershocks approach the "critical" (for impact on urban development) area of 156°–158°E. This observation is alarming, given the extent of damage to residential and non-residential buildings in Severo-Kurilsk after the main shock on July 29 (30).

To ensure the integrity of the experiment, the authors assessed the earthquake impact not only on the monitored site but also on the permanent Severo-Kurilsk seismic station. In both cases, calculations were based on accelerometer data. The Severo-Kurilsk seismic station's instruments are installed in a specialized 27 m^2 seismic pavilion on a concrete pedestal consisting of four 1.5 m × 1.5 m × 2.0 m pillars reinforced with pipes buried in the ground. Figure 8 shows a diagram of the magnitude–intensity relationship, taking into account the distance from Severo-Kurilsk to the earthquake epicenter. As can be seen from the figure, for distant seismic events (blue markers) with large magnitudes ($M \geq 6.0$), the difference in instrumental intensity between the ESS and SKR is virtually negligible. Similarly, there is virtually no difference for nearby events (red markers) with small magnitudes. Moreover, the impact of low-magnitude events is often more pronounced at the Severo-Kurilsk seismic station, which is not the case for events occurring 51–250 km away (blue and green markers on the graphs) from Severo-Kurilsk with magnitudes of

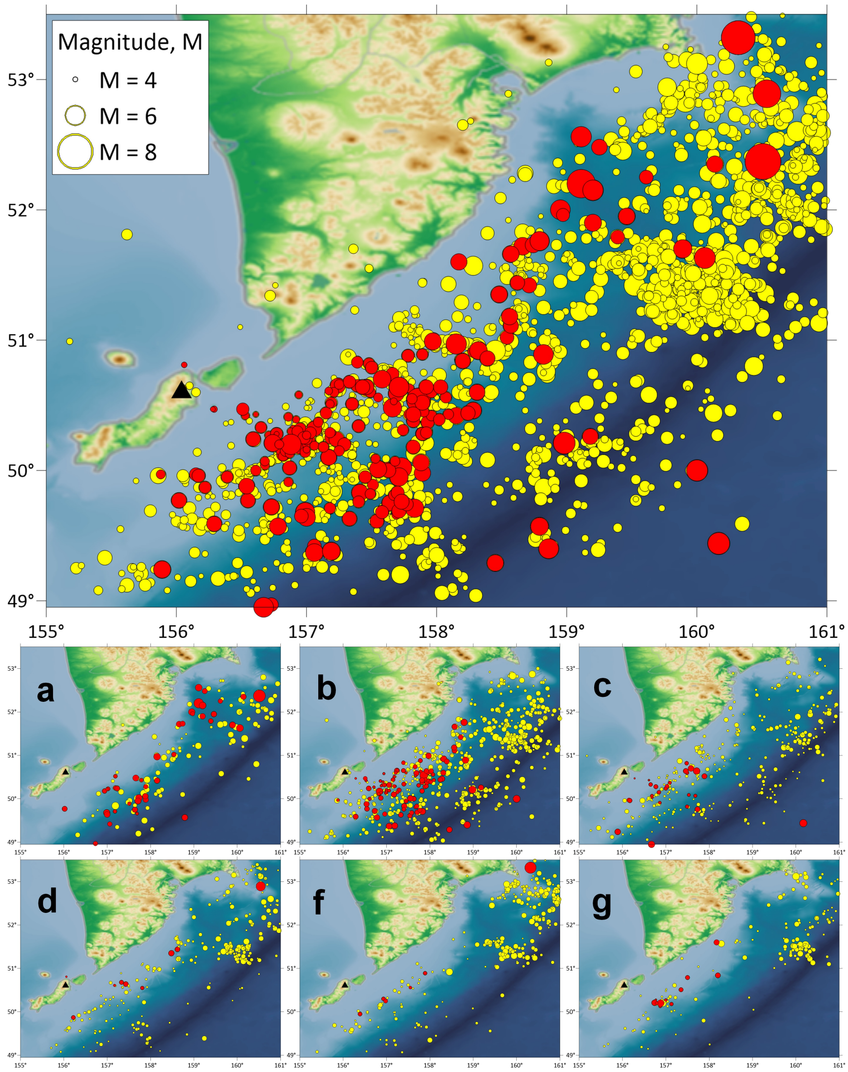

Figure 5. All seismic events recorded by Severo-Kurilsk seismic station from July 29, 2025 to October 15, 2025 (upper part of the figure); the lower part of the figure shows the distribution of aftershocks by the time of their occurrence: (*a*) from July 29 to 30, (*b*) from July 31 to August 15, (*c*) from August 16 to August 31, (*d*) from September 1 to September 15, (*e*) from September 16 to September 30, (*f*) from October 1 to October 15.

M = 3.5–5.5. Such earthquakes have a much stronger impact on the ESS than on the instruments installed on the Severo-Kurilsk seismic station pedestal.

The authors made an attempt to estimate the direction of the main shock and some of its aftershocks by determining the parameters of earthquake focal mechanisms that characterize the destruction process: the type of movement, the orientation of the rupture plane in space and the direction of the acting stresses. For the strongest seismic events, using a combination of local, regional, and global networks, the authors determined the mechanisms of the mainshock and some of its aftershocks over the observed period. The mechanism parameters are presented in Table 1. Data from the European-Mediterranean Seismological Center (EMSC) were used to calculate the mechanisms, as information on earthquake parameters was obtained from https://www.emsc-csem.org/Earthquake_information/.

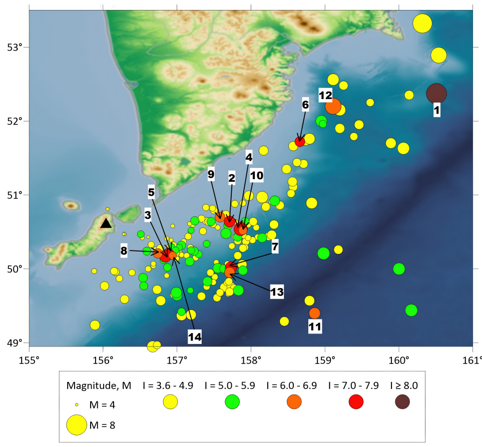

№	Date (Sakhalin)	Time (Sakhalin)	Latitude, °N	Longitude, °E	M	Δ, km	I, ESS
1	2025-07-30	10:24:50	52.37	160.51	8.3	366	9.1
2	2025-08-27	14:49:49	50.64	157.71	5.9	112	7.7
3	2025-08-02	07:07:54	50.17	156.84	6.0	75	7.6
4	2025-08-03	16:37:55	50.54	157.86	6.5	124	7.1
5	2025-10-11	23:25:57	50.20	156.88	6.0	75	7.1
6	2025-07-30	10:36:03	51.72	158.66	5.6	214	7.0
7	2025-07-31	01:47:42	50.02	157.73	6.0	135	7.0
8	2025-10-10	22:16:01	50.21	156.74	5.5	67	6.5
9	2025-08-23	14:44:15	50.70	157.58	5.6	103	6.4
10	2025-08-25	15:05:59	50.52	157.89	5.2	126	6.4
11	2025-07-31	16:27:13	49.40	158.86	5.9	241	6.3
12	2025-07-30	10:25:43	52.20	159.11	7.2	270	6.1
13	2025-07-31	03:57:34	49.95	157.71	5.7	138	6.1
14	2025-07-30	18:42:26	50.18	156.94	5.0	79	6.0

Figure 6. All perceptible earthquakes for the observed period with gradation by a certain instrumental intensity – on the left and a list of earthquakes with $I \geq 6.0$ – on the right. *Note:* M_L is the local Richter magnitude adopted in the practice SB GS RAS; the earthquakes in the table are presented from the operational catalog of the Yuzhno-Sakhalinsk Regional Operational Center.

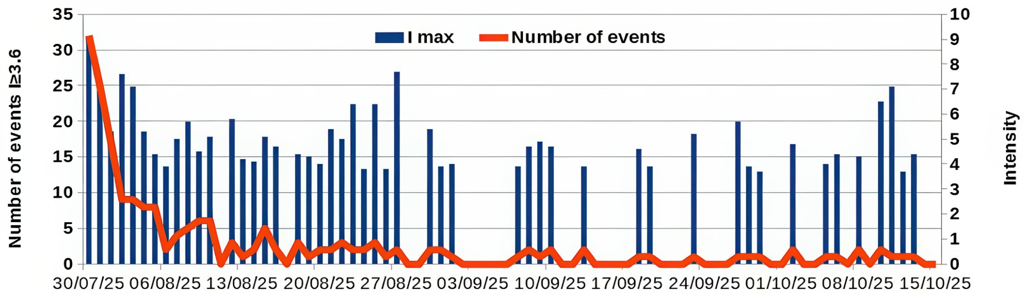

Figure 7. Diagram of the distribution of perceptible (from $I \geq 3.6$) events by time for the observed period from July 30 to October 15, 2025 (Sakhalin dates).

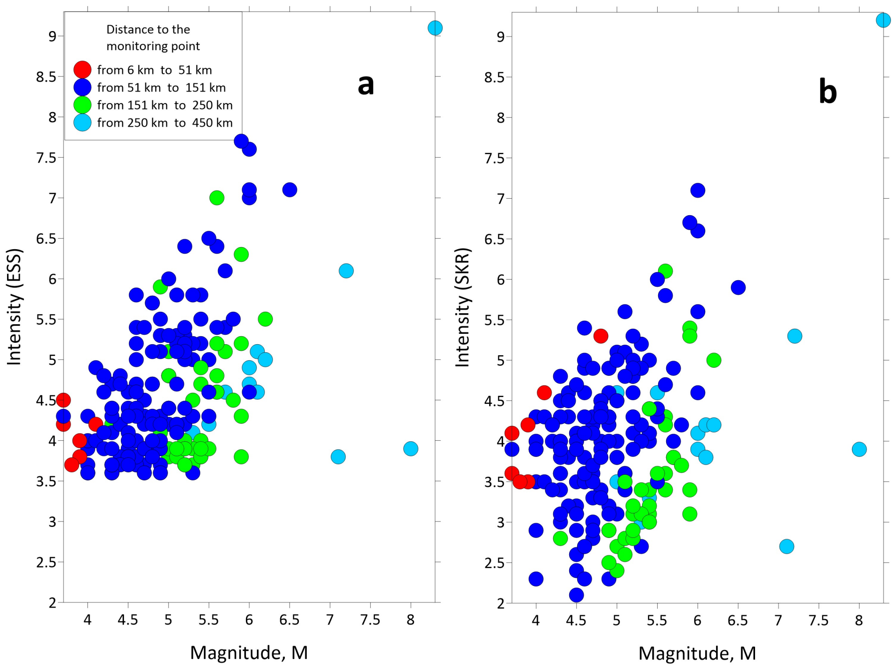

Figure 8. Diagram of the dependence of points on magnitude taking into account the distance, on the left – ESS, on the right – Severo-Kurilsk seismic station.

Table 1. Parameters of earthquake focal mechanisms – the main shock of July 29, 2025 UTC and some of its aftershocks (decision of the SB GS RAS)

No.	Earthquake parameters	Principal stress axes				Nodal planes						Stereogram of mechanisms (lower hemisphere)
		T		*P*		NP1			NP2			
		PL	Az	PL	Az	STK	DP	SLIP	STK	DP	SLIP	
1	2025-07-29 23:24 UTC $M_W = 8.8$	50	308	33	168	61	81	70	307	22	154	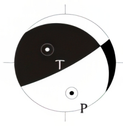
2	2025-07-29 23:37 UTC $M_W = 6.0$	72	224	15	9	85	31	71	287	61	102	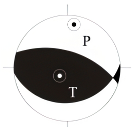
3	2025-07-30 01:03 UTC $M_W = 5.8$	5	268	85	88	358	40	−90	178	50	−90	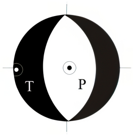
4	2025-07-30 14:47 UTC $M_W = 6.4$	40	115	3	208	259	61	28	154	66	147	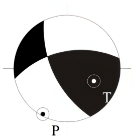
5	2025-07-30 16:57 UTC $M_W = 5.6$	4	181	60	84	117	56	−53	243	48	−132	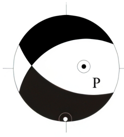
6	2025-07-31 03:48 UTC $M_W = 4.6$	4	56	60	318	351	56	−53	117	48	−132	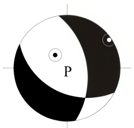
7	2025-07-31 05:27 UTC $M_W = 5.9$	11	123	16	217	259	70	−4	351	87	−160	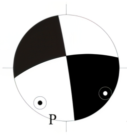
8	2025-07-31 06:51 UTC $M_W = 5.4$	27	21	27	126	164	50	0	74	89	140	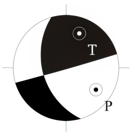
9	2025-07-31 14:34 UTC $M_W = 5.5$	75	9	15	189	99	60	90	279	30	90	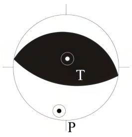
10	2025-08-01 18:20 UTC $M_W = 6.1$	45	349	45	169	79	90	90	169	0	0	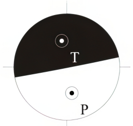
11	2025-08-01 20:07 UTC $M_W = 5.6$	54	307	34	106	158	14	45	25	80	100	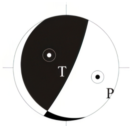

Continued on next page

Table 1. Parameters of earthquake focal mechanisms – the main shock of July 29, 2025 UTC and some of its aftershocks (decision of the SB GS RAS)(Continued)

No.	Earthquake parameters	Principal stress axes				Nodal planes						Stereogram of mechanisms (lower hemisphere)
		T		*P*		NP1			NP2			
		PL	Az	PL	Az	STK	DP	SLIP	STK	DP	SLIP	
12	2025-08-03 05:37 UTC $M_W = 6.8$	5	134	69	31	61	53	−65	203	44	−120	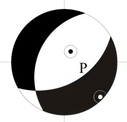
13	2025-08-06 20:27 UTC $M_W = 5.3$	14	209	26	306	345	61	−9	79	83	−151	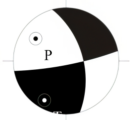
14	2025-08-09 14:04 UTC $M_W = 6.0$	22	60	32	164	199	51	−8	294	84	−140	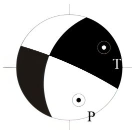
15	2025-08-12 04:15 UTC $M_W = 4.7$	25	339	65	159	249	70	−90	69	20	−90	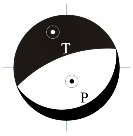
16	2025-08-19 14:41 UTC $M_W = 4.9$	23	153	58	287	277	28	−43	47	71	−111	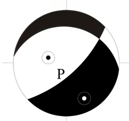
17	2025-08-23 03:44 UTC $M_W = 5.5$	63	323	25	118	187	22	63	37	70	101	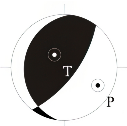
18	2025-08-25 04:06 UTC $M_W = 4.9$	45	217	30	91	337	81	60	233	31	163	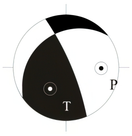
19	2025-08-25 06:48 UTC $M_W = 6.1$	72	9	15	224	126	61	78	329	31	109	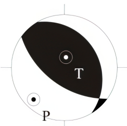
20	2025-08-27 03:49 UTC $M_W = 5.9$	45	339	45	159	69	90	90	159	0	0	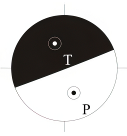
21	2025-09-13 02:37 UTC $M_W = 7.4$	65	339	25	159	69	70	90	249	20	90	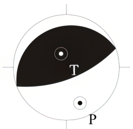
22	2025-09-18 18:58 UTC $M_W = 7.8$	57	43	13	153	210	41	41	87	64	124	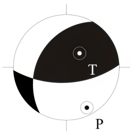

The focal mechanisms of the July 29, 2025, earthquake and some of its aftershocks were determined by the authors using the FOCMEC computational module integrated into the SEISAN seismological software suite [*SEISAN...*, 2011]. The arrival signs of the first *P*-wave movements recorded in the vertical component of seismic records were used to construct the earthquake definition. The data obtained by the authors do not contradict the data of other seismological agencies.

Figure 9 shows the earthquake epicenters with their ordinal numbers from Table 1 of the seismic events whose focal mechanisms were calculated. The color scheme also indicates the directions of the axes of maximum impact according to the ESS data (*a*) and according to the Severo-Kurilsk seismic station data (*b*). Epicenters shaded in blue indicate an east–west (EW) impact direction, green markers indicate a north–south (NS) impact direction, and red indicates vertical impact.

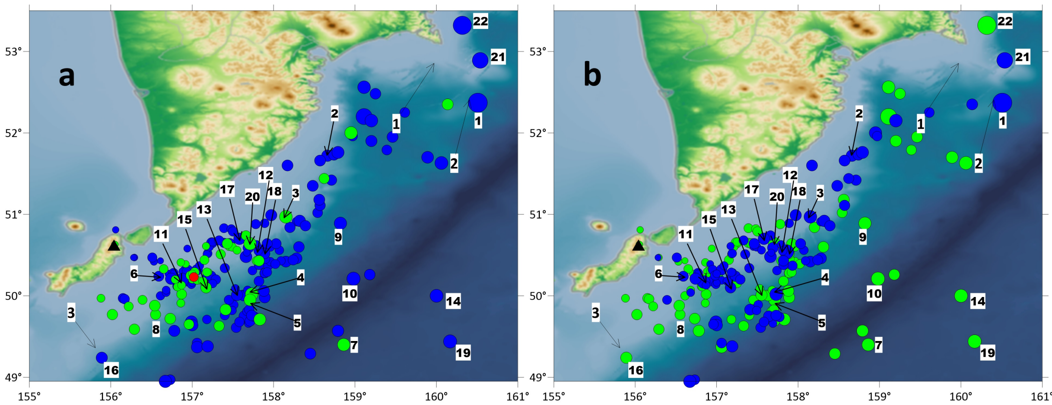

Figure 9. Directions of the axes of maximum impact according to the ESS data (*a*) and according to the Severo-Kurilsk seismic station data (*b*). The epicenters shaded with blue markers have an east–west (EW) impact direction, those shaded with green markers have a north–south (NS) impact direction, and those shaded with red markers have a vertical impact.

As can be seen from the figure, only one earthquake had a vertical impact on the monitoring object; all other noticeable seismic events had either an EW or NS impact direction. Unfortunately, the focal mechanisms constructed for only a few earthquakes cannot provide the authors with a complete picture of the source model for the July 29 (30) 2025 earthquake. However, when analyzing the directions of the axes of maximum impact from 195 noticeable aftershocks, it can be stated that the data obtained by the authors are completely consistent with the presented model of the rupture surface of the earthquake in Kamchatka on July 29, 2025, based on satellite geodesy and interferometry data [*Mikhailov et al.*, 2025]. According to the presented model, the main displacements on the fault surface (up to 11.5 m) were recorded in the southern Kamchatka Peninsula, as well as near the islands of Shumshu and Paramushir, and were directed horizontally toward the ocean trench (to the southeast).

As is well known, the most dangerous axis of impact on buildings during an earthquake is a horizontal (lateral) load directed perpendicular to the long axis of the building. The structures of most buildings are designed to withstand enormous vertical loads, but are much less resistant to shear loads. Impact along the short axis (across the building) is particularly dangerous, as it has fewer support points to resist bending. Most multi-story (and multi-entrance) buildings in Severo-Kurilsk (including the monitoring site) are oriented southeast to northwest along an axis of 135°–315°, which essentially coincides with the direction of displacement. Therefore, the displacement that occurred along the long axis of the buildings caused much less damage than if the impact had been along an axis oriented 45°–225°.

Consequently, the movement at the epicenter of the earthquake was directed not towards Paramushir Island from the coast of the Kamchatka Peninsula, but from Paramushir Island in a southeasterly direction (along the longitudinal axis of the main multi-story buildings in the city of Severo-Kurilsk), which made it possible to avoid catastrophic destruction and casualties.

4. Conclusion

The July 29 (30), 2025, M_W 8.8 earthquake that occurred near the Kamchatka Peninsula was a powerful seismic event, with macroseismic effects affecting not only the Kamchatka Peninsula but also Paramushir Island in the Sakhalin Region, whose only settlement is Severo-Kurilsk (population: approximately 2,500). Data obtained from the engineering seismometric station of the SB GS RAS, installed in a city building in Severo-Kurilsk, were comparable with data from a stationary station, which made it possible to collect detailed information on the nature of seismic impacts on this structure. The data obtained demonstrates that the integration of such systems into the urban environment is a key factor in minimizing risks and making prompt decisions to mitigate the consequences of powerful earthquakes. Based on the operational response to the intensity of shaking and the impact on the residential building, sent by the SB GS RAS in the form of summaries and reports to interested departments, municipal authorities and the developer, a continuous survey of the condition of the residential premises of the building and its supporting structure is conducted.

Acknowledgments. The work was supported by the Ministry of Science and Higher Education of the Russian Federation. The data used in the work were obtained with large-scale research facilities "Seismic Infrasound Array for Monitoring Arctic Cryolitozone and Continuous Seismic Monitoring of the Russian Federation, Neighbouring Territories and the World".

References

Aptikaev F. F., Erteleva O. O., Berzhinsky Yu. A., et al. Project of a new Russian seismic scale // Engineering Survey. — 2011. — No. 10. — P. 62–71. — (In Russian).

Chebrov D. V. The Mw = 8.8 Kamchatka megathrust earthquake of july 29, 2025 // Bulletin of Kamchatka Regional Association «Educational-Scientific Center». Earth Sciences. — 2025. — 3(67). — P. 113–117. — https://doi.org/10.31431/1816-5524-2025-3-67-113-117 — (In Russian).

Chebrov D. V., Droznin D. V., Matveenko D. V., et al. Prototype of a system for monitoring actual seismic impacts on buildings and structures of Petropavlovsk-Kamchatsky based on instrumental data // Problems of complex geophysical monitoring of seismoactive regions: Proceedings of the Eighth All-Russian scientific-technical conference with international participation, Petropavlovsk-Kamchatsky, September 26 - October 2, 2021. — Petropavlovsk-Kamchatsky : GS RAS, 2021. — P. 372–377. — https://doi.org/10.35540/903258-451.2021.8.70 — (In Russian).

Chebrov V. N., Gusev A. A., Gusyakov V. K., et al. Concept for developing a seismologic observation system for tsunami warning in the Russian Far East // Seismic Instruments. — 2010. — Vol. 46, no. 3. — P. 275–285. — https://doi.org/10.3103/s0747923910030096

Droznin D. V., Chebrov D. V., Droznina S. Y., et al. Automated Estimation of Seismic Shaking Intensity from Instrumental Data in Quasi-Real-time Mode and Its Use in the Operation of the of Seismic Early Warning Service in the Kamchatka Region // Seismic Instruments. — 2018. — Vol. 54, no. 3. — P. 239–246. — https://doi.org/10.3103/s0747923918030088

Droznin D. V. and Droznina S. Y. Interactive DIMAS program for processing seismic signals // Seismic Instruments. — 2011. — Vol. 47, no. 3. — P. 215–224. — https://doi.org/10.3103/s0747923911030054

Guryev V. V., Dorofeev V. M. and Bulykin V. I. Engineering Seismometric Monitoring for Calculation Structures,Prediction of Seismic Resistance and Maintenance Civil Objects in Operation // Academia. Architecture and Construction. — 2023. — No. 3. — P. 119–131. — https://doi.org/10.22337/2077-9038-2023-3-119-131 — (In Russian).

Kostenko I. S., Zaytsev A. I. and Pelinovsky E. N. Tsunami on July 29 (30), 2025 in the Kamchatka-Kuril Zone: Instrumental Observation and Modeling // Doklady Earth Sciences. — 2025. — Vol. 525, no. 2. — https://doi.org/10.1134/s1028334x25608648

Kostylev D. V. Formation of a unified system for collecting seismological information in the Sakhalin Division GS RAS // Russian Journal of Seismology. — 2021. — Vol. 3, no. 1. — P. 41–53. — https://doi.org/10.35540/2686-7907.2021.1.03 — (In Russian).

Kostylev D. V. and Kostyleva N. V. Development of engineering seismic monitoring methods in seismically active regions using the example of seismometric stations on Shikotan Island // Physics of Geospheres. — Vladivostok : V.I. Il'ichev Pacific Oceanological Institute FEB RAS, 2025a. — P. 119–122. — https://doi.org/10.62994/dvo.2025.37.25.027 — (In Russian).

Kostylev D. V. and Kostyleva N. V. System of engineering seismometric observations on the Kuril Islands under conditions of constant intensive seismic impacts // Natural and technogenic risks. Safety of structures. — 2025b. — Vol. 81, no. 6. — P. 30–37. — (In Russian).

Kostylev D. V., Kostyleva N. V. and Shchukin M. A. Seismological data information system in the Sakhalin Branch of the GS RAS // Russian Journal of Seismology. — 2025. — Vol. 7, no. 4. — P. 46–59. — https://doi.org/10.35540/2686-7907.2025.4.06 — (In Russian).

Medvedev S., Sponheuer W. and Kárník V. Neue seismische Skala // 7. Tagung der Europäischen Seismologischen Kommission vom 24.9. bis 30.9. 1962 in Jena, DDR. — De Gruyter, 1964. — P. 69–76. — https://doi.org/10.1515/9783112756430-019

Mikhailov V. O., Konvisar A. M., Smirnov V. B., et al. The Rupture Surface Model of the July 29, 2025 Mw 8.8 Kamchatka Earthquake Based on Satellite Geodesy and Interferometry Data // Doklady Earth Sciences. — 2025. — Vol. 525, no. 2. — https://doi.org/10.1134/s1028334x25608752

Mishatkin V. N., Zakharchenko N. Z. and Chebrov V. N. Hardware for the seismic subsystem of the tsunami warning service // Seismic Instruments. — 2012. — Vol. 48, no. 1. — P. 16–33. — https://doi.org/10.3103/s0747923912010100

SEISAN Earthquake analysis software for Windows, Solaris, Linux and Macosx. Version 9.0.1 / ed. by L. Ottemöller, P. Voss and J. Havskov. — SEISAN, 2011.

Titov E. Yu., Agafonov V. M., Neeshpapa A. V., et al. Measuring complexes to monitor railway facilities in seismically hazardous regions // Put' i Putevoye Khozyaystvo. — 2021. — No. 2. — P. 27–31. — (In Russian).